Solving Linear Diffusion-Reaction Networks in Porous Catalyst Particles Using BEM

Sriganesh R. Karur and P. A. Ramachandran
Dept. of Chemical Engineering, Washington University, St. Louis, MO 63130

Multiple diffusion reactions are frequently encountered in the modeling of heterogeneous catalytic reactors. Obtaining an accurate estimate of the yield and selectivity in such reactions is crucial for an optimal design of reactors. Due to the inadequacy of analytical techniques in handling nonuniform catalyst shapes and mixed boundary conditions, numerical techniques are often employed to compute these design parameters. Among other numerical techniques, the boundary element method (BEM) is a superior method to solve linear diffusion reaction problems. The integral nature of the BEM formulation allows for boundary-only discretization of the particle, thus reducing the computer execution time and the data preparation effort. A boundary element algorithm is developed to solve a network of linear diffusion reactions in porous catalyst particles in two dimensions. For this purpose, a matrix of fundamental solutions is defined and derived. The developed algorithm is applied to complex reaction networks to obtain the yield of intermediates for nonregular catalyst shapes and nonuniform boundary conditions. The method can be used as a design tool to study particle scale modeling in detail and can be incorporated into an overall reactor model.

Introduction

The quantitative understanding of the diffusion reaction phenomena in a catalyst particle is essential for the optimal design of heterogeneous reactors. Reaction systems of industrial importance often involve multiple species participating in a complex network of reactions with nonlinear kinetics. The study of reaction networks with linear kinetics (Wei and Prater, 1962) is a prerequisite for detailed analysis of networks with nonlinear kinetics. Also the linear approximation in itself could be a reasonable assumption for practical applications in view of the complexity of the system. For example, a network of linear reactions is used as a "lumped" kinetic model for the process of catalytic cracking in petroleum industry (Stangeland and Kittrel, 1972). Even with this linear approximation, the estimation of the key design parameters such as the yield and the selectivity is a challenging task unless the catalyst geometry is regular (like slab, cylinder, and sphere) and the boundary conditions are uniform.

Mathematically, a network of linear diffusion reactions in a porous catalyst particle can be expressed in vector notation as

$$\nabla^2 \mathbf{c} = \tilde{K}\mathbf{c} \quad \text{in} \quad \Omega, \tag{1}$$

where $\mathbf{c}$ is the vector of concentrations of N independent species participating in the reaction, $\tilde{K}$ is the matrix consisting of the "composite" rate constants (ratio of reaction rate constants to the diffusion coefficients), and Ω is the domain of the catalyst particle. The set of governing differential equations are coupled because matrix $\tilde{K}$ is typically not a diagonal matrix. The domain Ω is the volume (surface) of the catalyst particle in the 3-D (2-D) case. The boundary conditions are specified over the enclosing surface (perimeter), Γ, in the 3-D (2-D) case. The analytical solution for the preceding vector equation is difficult to obtain due to coupled reactions, nonregular catalyst geometry, and nonuniform boundary conditions. Hence there is a need to develop effective numerical techniques to solve such equations to get an estimate of the product distribution. Among several numerical methods, the boundary element method (BEM) is an elegant technique to solve linear diffusion reaction equation (Brebbia and Dominguez, 1989; Ramachandran, 1993). In the recent past the BEM has found widespread use in fluid dynamic problems (e.g., Pozrikidis, 1992; Power and Partridge, 1994). But the method has not yet made an impact in the field of chemical reaction engineering.

Using BEM the differential Eq. 1 can be converted to an equivalent integral equation by applying the Green–Gauss theorem. Owing to the integral nature of the resulting formulation, the dimensionality of the problem is reduced by one, that is, the solution over the entire domain is obtained by discretizing the boundary of the particle. Since only the boundary is discretized, handling complex geometries and imposing nonuniform boundary conditions becomes simple. This significantly reduces the degrees of freedom (number of variables required to obtain a numerical solution to Eq. 1) when compared to other numerical techniques like the finite difference method and the finite element method. Ramachandran (1991) has demonstrated the use of BEM for solving a single linear diffusion reaction equation in a catalyst particle with nonuniform boundary conditions. However, the method has not yet been applied to solve multiple diffusion reaction equations. In this article, we extend the boundary element procedure to solve such coupled multiple linear diffusion reaction equations. For this purpose, the governing differential equations are formulated in a vector form and the *matrix of fundamental solutions* is defined. The *matrix of fundamental solutions* is the tensor analog of the scalar fundamental solution used in single reactions and is obtained by using matrix transformation techniques. The algorithm developed here can be used to study the effect of catalyst shape and nonuniform boundary conditions on the yield of a desired product in a complex reaction network. Illustrations to this effect are presented in this article.

The outline of the article is as follows: the next section discusses the mathematics of the boundary element method. The third section describes the procedure to obtain the *matrix of fundamental solutions* along with an illustration. The fourth section demonstrates the usefulness of the developed algorithm with some numerical examples. The final section presents a brief summary of this research work.

Boundary Element Method

The mathematics of the boundary element method for both single and multiple reactions is discussed in this section. We review the method for single reactions first since the extension of the boundary element procedure to multiple reactions essentially involves an approach parallel to that of the single reaction case.

Single reaction

Consider the single irreversible reaction $A \xrightarrow{m_1^2} B$. The governing partial differential equation can be expressed as

$$\nabla^2 c - m_1^2 c = 0, \tag{2}$$

where ∇^2 is the Laplacian operator, c is the dimensionless concentration variable of species A, and m_1^2 is the "composite" rate constant. The idea behind BEM is to convert this differential problem into an integral problem by applying the method of weighted residuals and the Green–Gauss theorem.

The first step in BEM is to multiply Eq. 2 with a weighting function and integrate the resultant over the entire domain. Thus the weighted residual formulation becomes

$$\int_\Omega G\,(\nabla^2 c - m_1^2 c)\,d\Omega = 0, \tag{3}$$

where G is the weighting function and Ω is the domain (surface for 2-D problems) under consideration. The next step in BEM is to use the Green–Gauss theorem (i.e., integration of Eq. 3 by parts twice) to obtain the integral formulation:

$$\int_\Gamma \left(G\frac{\partial c}{\partial n} - c\frac{\partial G}{\partial n} \right) d\Gamma + \int_\Omega c(\nabla^2 G - m_1^2 G)\,d\Omega = 0, \tag{4}$$

where Γ is the boundary of the catalyst particle. Notice that the second-order derivatives (∇^2) on the dependent variable, c, in Eq. 3 is transferred to the weighting function, G, in Eq. 4. The dimensionality of the problem with respect to the dependent variable can be reduced by one if the domain integral in Eq. 4 can be eliminated. This is achieved by choosing G as the solution to the following equation:

$$\nabla^2 G - m_1^2 G = -\,\delta(x-\xi, y-\eta), \tag{5}$$

where $\delta(x-\xi,\ y-\eta)$ is the Dirac delta function applied at any source point (ξ,η). Physically, $-\delta$ represents a unit concentration source at the point (ξ,η). The solution to Eq. 5 yields the generalized Green's function or the fundamental solution to the diffusion reaction operator and is expressed as

$$G = \frac{1}{2\pi} K_0(m_1 r), \tag{6}$$

where K_0 is the modified Bessel function of the second kind, order zero, and r is the Euclidean distance between the source (ξ,η) and the field points (x,y). Using Eq. 5 and the sifting property of the delta function in Eq. 4, the final form of the integral formulation becomes

$$\int_\Gamma (Gp - Qc)\,d\Omega - d_i c_i = 0, \tag{7}$$

where p is the normal gradient of concentration, Q is the normal derivative of G, and d_i is a coefficient that depends on the location of the source point i on the boundary (Brebbia and Dominguez, 1989).

Equation 7 is solved by discretizing the boundary into sufficiently small elements and approximating the dependent variable using suitable basis functions. The dependent variables are either the concentrations, c, or their normal gradients, p, depending on the boundary conditions. The boundary conditions can be of the Dirichlet type (c specified), the Neumann type (p specified), or the Robin type (combination of c and p). By discretizing the boundary into small elements and imposing the boundary conditions, the integral formulation can be reduced to a system of linear algebraic equations of the form,

$$\tilde{A}\boldsymbol{x} = \boldsymbol{B}, \tag{8}$$

where $\tilde{A}$ is the coefficient matrix, $\boldsymbol{x}$ and $\boldsymbol{B}$ are the unknown and known vectors, respectively. This equation is solved for the unknown boundary variables, $\mathbf{x}$ by a standard linear equation solver. The procedure for single reaction is well established and discussed in detail by Ramachandran (1991). In the following subsection we show the extension of this approach to handle multiple reactions by defining the *matrix of fundamental solutions*.

Multiple reactions

For multiple linear reactions (both reversible and irreversible), diffusion reaction equations similar to Eq. 2 can be written for each independent species. Equation 1, which is the vector analog of the single diffusion reaction equation, is rewritten as

$$\nabla^2 \mathbf{c} - \tilde{K}\mathbf{c} = 0 \tag{9}$$

where $\mathbf{c}$ is the concentration vector whose dimension is the total number of independent species and $\tilde{K}$ is the "composite" rate constant matrix. The nature of $\tilde{K}$ matrix depends upon the complexity of the network. Analogous to the fundamental solution to the single reaction case, we define the *matrix of fundamental solutions* for multiple reactions denoted as $\tilde{G}$. Using this $\tilde{G}$ matrix as the weighting function, the weighted residual formulation for multiple reactions takes the form

$$\int_\Omega \tilde{G}\cdot(\nabla^2\mathbf{c} - \tilde{K}\mathbf{c})d\Omega = 0. \tag{10}$$

Here $\tilde{G}$ is an $(N \times N)$ matrix (N being the number of independent species). The components of the $\tilde{G}$ matrix are represented as a set of row vectors as follows:

$$\tilde{G} = \begin{pmatrix} \mathbf{G}_1^T \\ \mathbf{G}_2^T \\ \vdots \\ \mathbf{G}_N^T \end{pmatrix}. \tag{11}$$

The row vectors, $\mathbf{G}_k^T$, are the transpose of the fundamental solution vector, $\mathbf{G}_k$, corresponding to the kth species. Our primary objective is to judiciously choose the $\tilde{G}$ matrix such that the integral formulation (Eq. 10) does not contain any domain integral. To attain our goal let us consider the weighted residual formulation corresponding to the kth component of Eq. 10:

$$\int_\Omega \mathbf{G}_k^T\cdot(\nabla^2\mathbf{c} - \tilde{K}\mathbf{c})d\Omega = 0. \tag{12}$$

Applying the Green–Gauss theorem to Eq. 12, we arrive at the integral formulation:

$$\int_\Gamma \left(\mathbf{G}_k^T\cdot\frac{\partial \mathbf{c}}{\partial n} - \frac{\partial \mathbf{G}_k^T}{\partial n}\cdot\mathbf{c}\right)d\Gamma - \int_\Omega (\nabla^2\mathbf{G}_k^T\cdot\mathbf{c} - (\mathbf{G}_k^T\tilde{K})\cdot\mathbf{c})d\Omega = 0. \tag{13}$$

Rearranging the domain integral term of Eq. 13 by using matrix operations, the integral formulation becomes

$$\int_\Gamma \left(\mathbf{G}_k^T\cdot\frac{\partial \mathbf{c}}{\partial n} - \frac{\partial \mathbf{G}_k^T}{\partial n}\cdot\mathbf{c}\right)d\Gamma - \int_\Omega \left\{[\nabla^2\mathbf{G}_k - (\tilde{K}^T\mathbf{G}_k)]^T\cdot\mathbf{c}\right\}d\Omega = 0. \tag{14}$$

The domain integral in Eq. 14 can be eliminated by choosing $\mathbf{G}_k$ to be the *fundamental solution vector* to the diffusion reaction operator in vector form

$$\nabla^2\mathbf{G}_k - (\tilde{K}^T\mathbf{G}_k) = -\mathbf{e}_k\delta(\mathbf{x}_i), \tag{15}$$

where $\mathbf{e}_k$ are the orthogonal unit vectors in the composition space and $\mathbf{x}_i$ is the source point vector. For example, in a three-component system (i.e., where three independent diffusion reaction equations can be written), the $\mathbf{e}_k$ vector is given by

$$e_1 = (1,0,0) \quad e_2 = (0,1,0) \quad e_3 = (0,0,1). \tag{16}$$

Using Eq. 15 and the sifting property of the Dirac delta function, in Eq. 14, the integral formulation is reduced to the computation of boundary integrals alone:

$$\int_\Gamma (\mathbf{G}_k^T\cdot\mathbf{p} - \mathbf{Q}_k^T\cdot\mathbf{c})d\Gamma - d_i c_k(\mathbf{x}_i) = 0, \tag{17}$$

where the coefficient d_i depends as usual on the location of the source point. The preceding equation corresponds to the kth independent species. Writing similar equations for all the N species, that is, for $k = 1$ to N, we obtain the vector form of the integral formulation:

$$\int_\Gamma (\tilde{G}\mathbf{p} - \tilde{Q}\mathbf{c})d\Gamma - \tilde{d}_i\mathbf{c}(\mathbf{x}_i) = 0, \tag{18}$$

where $\tilde{Q}$ is the normal derivative of $\tilde{G}$ and can be easily determined once $\tilde{G}$ is known, and $\tilde{d}_i$ is the matrix containing the geometry-dependent coefficients (Brebbia and Dominguez, 1989). Equation 18 is the integral formulation for multiple reactions and is a generalization of Eq. 7 that is applicable for single reactions. The integral equation (Eq. 18) is discretized in a similar manner to the one described in the previous subsection and the boundary unknowns for all the independent species are solved simultaneously. The next section discusses the mathematical procedure to calculate the *matrix of fundamental solutions*, $\tilde{G}$.

Matrix of Fundamental Solutions

Derivation

The crucial step in the previous analysis is to evaluate the individual entries of the $\tilde{G}$ matrix. For that purpose let us consider the individual rows of the $\tilde{G}$ matrix. As mentioned in the subsection on multiple reactions, the *fundamental solution vector* $\mathbf{G}_k$ can be obtained by solving Eq. 15. But the solution is not simple because of the coupling effect of the $\tilde{K}^T$ matrix. In order to decouple this system of partial differential equations we use a matrix transformation technique and finally obtain a closed-form analytical expression for $\boldsymbol{G}_k$. The transformation used is of the form,

$$\boldsymbol{G}_k = \tilde{L}\boldsymbol{Y}_k, \tag{19}$$

where $\tilde{L}$ is the modal matrix obtained by arranging the independent eigenvectors of the $\tilde{K}^T$ matrix, columnwise, and $\boldsymbol{Y}_k$ is the new dependent vector variable in the ensuing decoupled system of differential equations.

The eigenvectors of the $\tilde{K}^T$ matrix ideally provide an orthogonal basis in the composition space and therefore enables us to decouple the complex network. Wei and Prater's (1962) discussion on this subject is extensive and is a classic reference on the mathematical analysis of a network of linear reactions. Substituting for $\boldsymbol{G}_k$ from Eq. 19 into Eq. 15, we get

$$\nabla^2 \tilde{L}\boldsymbol{Y}_k - \tilde{K}^T\tilde{L}\boldsymbol{Y}_k = -\boldsymbol{e}_k\delta(\boldsymbol{x}_i). \tag{20}$$

Premultiplying Eq. 20 by the inverse of the modal matrix, $\tilde{L}^{-1}$, we obtain

$$\nabla^2 \boldsymbol{Y}_k - (\tilde{L}^{-1}\tilde{K}^T\tilde{L})\boldsymbol{Y}_k = -\tilde{L}^{-1}\boldsymbol{e}_k\delta(\boldsymbol{x}_i). \tag{21}$$

By using the concept of similarity transformation, the bracketed term on the LHS of this equation reduces to a diagonal matrix containing the eigenvalues along the diagonal, thereby decoupling the linear network. The mth component, $(Y_k)_m$, of this vector equation for $\boldsymbol{Y}_k$ is therefore given by

$$\nabla^2 (Y_k)_m - \lambda_m (Y_k)_m = -L_{mk}^{-1}\delta(\boldsymbol{x}_i), \tag{22}$$

where λ_m is the eigenvalue or the spectrum of the mth component; and L_{mk}^{-1} is the element corresponding to the mth row and kth column of the $\tilde{L}^{-1}$ matrix. The partial differential equation (Eq. 22) is analogous to Eq. 5 for a single reaction. Therefore the corresponding solution for the scalar component $(Y_k)_m$ is given in the form of modified Bessel function of the second kind and order zero:

$$(Y_k)_m = \frac{1}{2\pi} L_{mk}^{-1} K_0\left(\sqrt{\lambda_m}\, r\right). \tag{23}$$

In the RHS of Eq. 23, the coefficient of the Bessel function, L_{mk}^{-1}, acts as a scaling parameter in the spectral space corresponding to the interaction between the mth and the kth species. We obtain the individual elements of the matrix of fundamental solutions, $(G_k)_l$, by substituting $(Y_k)_m$ in Eq. 19:

$$(G_k)_l = \sum_{m=1}^{N} L_{lm}(Y_k)_m = \sum_{m=1}^{N} \frac{1}{2\pi} L_{lm} L_{mk}^{-1} K_0\left(\sqrt{\lambda_m}\, r\right). \tag{24}$$

The mathematical procedure discussed in this subsection is applicable for the case when all the eigenvalues are distinct. It can be shown that, the eigenvalues of $\tilde{K}^T$ matrix is always greater than or equal to zero and the corresponding eigenvectors are linearly independent (Wei and Prater, 1962). Modification of the preceding analysis is necessary in two circumstances: (1) zero eigenvalue, and (2) multiplicity of eigenvalues. For the case of zero eigenvalue, the Bessel function kernel reduces to a logarithmic kernel in the limiting case. For the case of the multiplicity of eigenvalues, a small perturbation to the eigenvalues guarantees a feasible solution.

The developed algorithm is general in nature and can be applied to any network of linear diffusion reaction systems. The network can include both reversible and irreversible reactions. Although the computational implementation in the present work has been restricted to 2-D problems, similar analysis can be extended to 3-D problems. For the single-reaction case, the fundamental solution for the diffusion reaction operator in 3-D takes the form,

$$G_{3\mathrm{D}} = \frac{1}{4\pi r}\exp(-m_1 r). \tag{25}$$

The fundamental solution $G_{3\mathrm{D}}$ is the 3-D analog of G in Eq. 6. Using this fundamental solution, the 3-D *matrix of fundamental solutions*, $\tilde{G}_{3\mathrm{D}}$, can be derived and the diffusion reaction problem can be solved by discretizing the surface alone. Thus the BEM provides an elegant mathematical framework to solve a network of linear diffusion reactions very effectively. The next subsection provides an example to obtain the $\tilde{G}$ matrix for a series reaction network.

Note that the vector equation (Eq. 9) can be diagonalized directly by using a transformation similar to the one used for the Green's function. However, when Robin-type boundary conditions are imposed, the boundary conditions do not get decoupled. Hence the solution procedure using direct diagonalization is not general and restricted to problems with Dirichlet-type boundary conditions. In contrast, by using the *matrix of fundamental solutions* as developed here, the concentration variables and the boundary conditions are untouched and hence the implementation becomes general.

Example

To illustrate the theoretical development discussed in the preceding subsection, we consider the series irreversible reaction,

$$A \xrightarrow{m_1^2} B \xrightarrow{m_2^2} C.$$

Since the reactions are irreversible, the rate of reaction of A is essentially independent of the concentration of B. But the rate of reaction of B depends on the concentration of A as well as B. Thus the governing differential equation in vector form is

$$\begin{pmatrix} \nabla^2 c_A \\ \nabla^2 c_B \end{pmatrix} = \begin{pmatrix} m_1^2 & 0 \\ -m_1^2 & m_2^2 \end{pmatrix} \begin{pmatrix} c_A \\ c_B \end{pmatrix}, \tag{26}$$

where m_1^2 and m_2^2 are the "composite" rate parameters corresponding to the first and the second reactions, respectively. The eigenvalues of the $\tilde{K}^T$ matrix are m_1^2 and m_2^2 and the corresponding eigenvectors are (1, 0) and $[-m_1^2/(m_1^2 -$

m_2^2), 1]. Therefore the modal matrix $\tilde{L}$ and its inverse $\tilde{L}^{-1}$ are given by

$$\tilde{L} = \begin{pmatrix} 1 & \left(\dfrac{m_1^2}{m_1^2 - m_2^2}\right) \\ 0 & 1 \end{pmatrix} \tag{27}$$

$$\tilde{L}^{-1} = \begin{pmatrix} 1 & -\left(\dfrac{m_1^2}{m_1^2 - m_2^2}\right) \\ 0 & 1 \end{pmatrix}. \tag{28}$$

After $\tilde{L}$ and $\tilde{L}^{-1}$ are computed, the substitution of their individual elements in Eq. 24 results in the *matrix of fundamental solution,*

$$\tilde{G} = \frac{1}{2\pi} \begin{pmatrix} K_0(m_1 r) & 0 \\ \dfrac{m_1^2}{m_1^2 - m_2^2}[K_0(m_2 r) - K_0(m_1 r)] & K_0(m_2 r) \end{pmatrix}. \tag{29}$$

The preceding example shows that it is fairly straightforward to obtain the *matrix of fundamental solutions* for any given general linear network.

Results and Discussion

In this section we illustrate the usefulness of the technique developed in the previous section, as a design tool by considering a few numerical examples. In the two following subsections, we study the effect of catalyst geometry and nonuniform boundary conditions, respectively, on the yield of intermediate products in complex reaction networks.

Effect of catalyst shape

Several catalyst shapes like trilobes, quadrulobes, wagon wheels, and the like, are being used in the industry (Cooper et al., 1986; Sie, 1993) for a variety of chemical processes to improve the diffusional characteristics of the catalyst. Control of yield to a desired (undesired) product by altering the catalyst shape is known as catalyst tailoring and is increasingly being practiced in the industry. For tailoring the catalyst morphology efficiently, the numerical technique developed here is particularly useful. In this subsection we demonstrate the use of this technique to solve a complex linear reaction network (Figure 1) in some regular and nonregular catalyst shapes. The "composite" rate constants are chosen arbitrarily to illustrate the utility of the procedure. The governing differential equations for each independent species for the parameters in Figure 1 are given as

$$\nabla^2 c_A = 16 c_A \tag{30}$$

$$\nabla^2 c_B = -16 c_A + 8 c_B \tag{31}$$

$$\nabla^2 c_D = -5 c_B + 3 c_D \tag{32}$$

$$\nabla^2 c_F = -2 c_D + c_F. \tag{33}$$

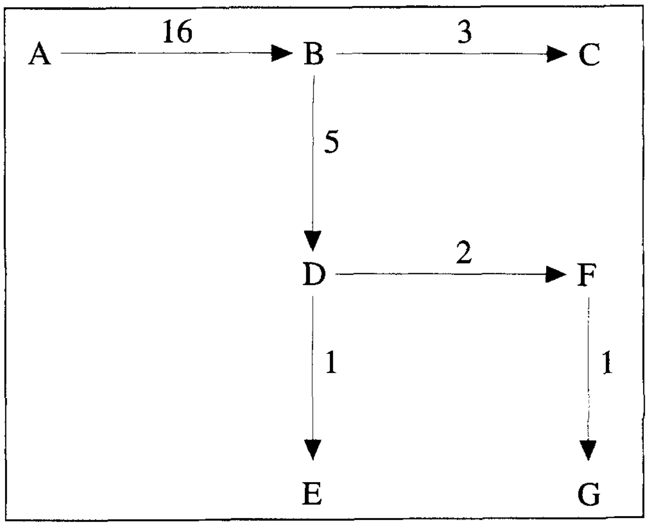

Figure 1. Reaction network 1.

Four catalyst shapes (three simply connected domains and one multiply connected domain) are selected to solve the network of linear diffusion reactions. In all the shapes shown in Figure 2 the characteristic length parameter, L, defined as the ratio of surface area to the perimeter of the particle [analogous to Aris's (1957) definition] is kept constant and a value of 0.25 is taken in this example. Depending on the location of the interpolating nodes, there are two ways of discretizing the boundary of the catalyst: (1) conforming elements where interpolating nodes are placed at the element end points, and (2) non-conforming elements where all the interpolating nodes are placed within the element. The difference between conforming and non-conforming elements is shown pictorially in Figure 3. In nonconforming elements the interpolating nodes are chosen to be the roots of the Legen-

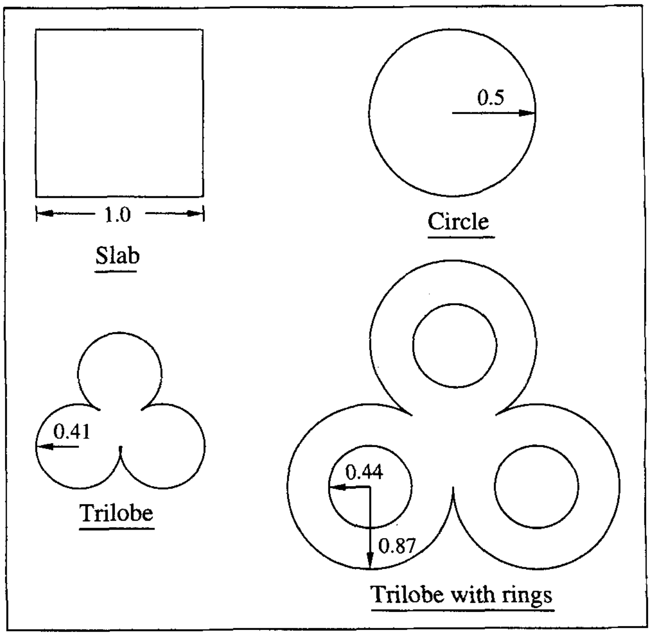

Figure 2. Different catalyst shapes examined in this study.

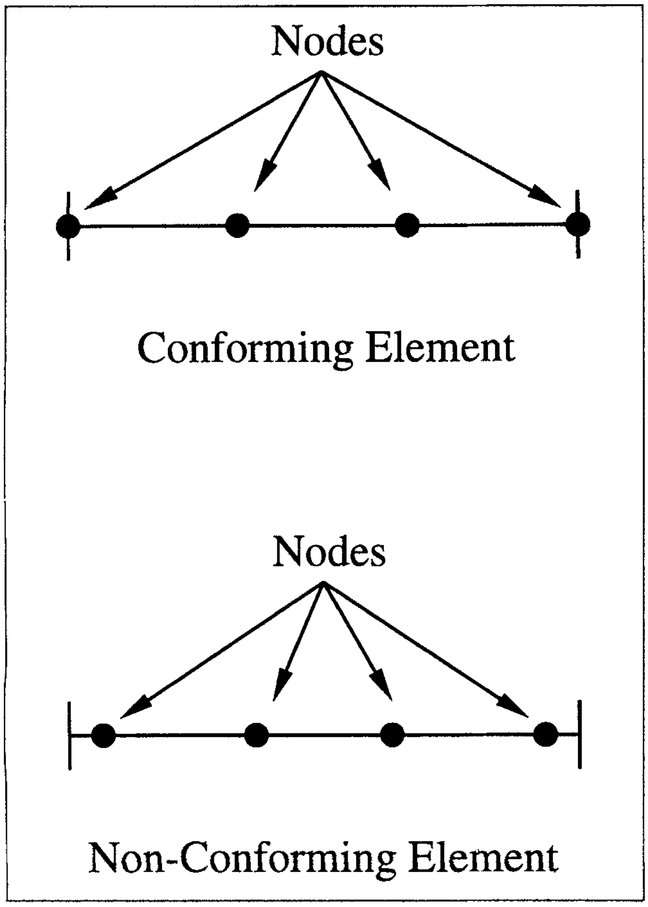

Figure 3. Node placement in conforming and nonconforming element discretization in BEM.

dre polynomial; in other words, they are located at the Gaussian quadrature points. Further details about the nonconforming elements and the procedure for node placement and error estimation can be found in Karur and Ramachandran (1995). The principal advantage in using nonconforming elements is that the singularities (arising due to geometry and boundary conditions) can be easily handled. In this work the boundary is discretized by nonconforming cubic elements. Throughout the perimeter of the catalyst, Dirichlet conditions are prescribed, that is, concentration of species A, B, D, and F are specified. Here $c_A = 1$ and $c_B = c_D = c_F = 0$ are used. The CPU time to execute the algorithm with 200 deg of freedom in an IBM Power Station 360 is approximately 15 s.

Yield of a product is defined as the ratio of the amount of that product exiting the catalyst to the amount of A entering the catalyst particle. Table 1 shows the values of the yield for each of the four catalyst shapes. The results indicate that for singly connected domains (slab, circle, and trilobe), there is no substantial difference in yields for the given set of rate parameters. However, when a multiply connected domain is considered, the results are different. The last row in Table 1 shows that in the trilobe catalyst with rings, the yield of D decreases by 20% with respect to the regular trilobe catalyst. If D is a by-product that has to be minimized in the production unit, then the use of the trilobe catalyst with rings is a better choice. Moreover due to larger particle size, the use of this catalyst in packed-bed reactors would reduce the pressure drop considerably (Cooper et al., 1986). Similar studies can be performed to evaluate several catalyst shapes in order to achieve the desired yield of a particular product. Although the reaction scheme considered here is arbitrary, the computational procedure can be used advantageously in realistic kinetics. High accuracy, ease of mesh generation, and the "boundary only" discretization makes this method a valuable tool to perform a systematic study of catalyst shapes.

Table 1. Yield of Intermediates for Different Catalyst Shapes

Catalyst	B	D	F
Slab	0.8267	0.0944	0.0083
Circle	0.8370	0.0914	0.0070
Trilobe	0.8275	0.0990	0.0070
Trilobe with rings	0.8482	0.0800	0.0067

Effect of nonuniform boundary conditions

The boundary element technique is versatile in handling problems with nonuniform boundary conditions. One such case occurs in a trickle-bed reactor when the external surface of the catalyst is only partly covered by the flowing liquid (rivulet). This phenomenon is called the *partial wetting effect* and has been the subject of active research for over a decade (Ramachandran and Smith, 1979; Mills and Duduković, 1979; Yentekakis and Vyenas, 1987; Funk et al., 1988; Harold, 1993, among others). Partial wetting leads to particle scale nonuniformities that have an important bearing on the reactor performance. The computational methodology developed in this work can be used to evaluate the prediction of single- and multiple-rivulet models for trickle-bed reactors and to study the parametric sensitivity to particle scale nonuniformities. We demonstrate the use of the developed algorithm by examining the effect of different wetting configurations on the yield of intermediates for the same degree of external wetting in a square catalyst pellet. For 50% external wetting, four different configurations are considered (Figure 4). Dirichlet and Neumann boundary conditions are prescribed on the wetted and-nonwetted regions, respectively.

A more general reaction network as shown in Figure 5 is chosen to demonstrate the capability of the technique to handle complex networks. Many reaction schemes of industrial relevance can be modeled using a truncated version of this reaction network. For the parameters shown in Figure 5 the governing partial differential equations are given by

$$\nabla^2 c_A = 39c_A - 2c_B - c_C - c_D \tag{34}$$

$$\nabla^2 c_B = -25c_A + 16c_B - 2c_C - c_D \tag{35}$$

$$\nabla^2 c_C = -4c_A - 6c_B + 9c_C - 6c_D \tag{36}$$

$$\nabla^2 c_D = -9c_A - 4c_B - 3c_C + 9c_D. \tag{37}$$

Again, cubic nonconforming elements are used to discretize the boundary of the catalyst particle. The discretization for each configuration is different because more elements need to be placed near the Dirichlet–Neumann singularity (Karur and Ramachandran, 1995). From Table 2, we observe that the yield of intermediates change with different

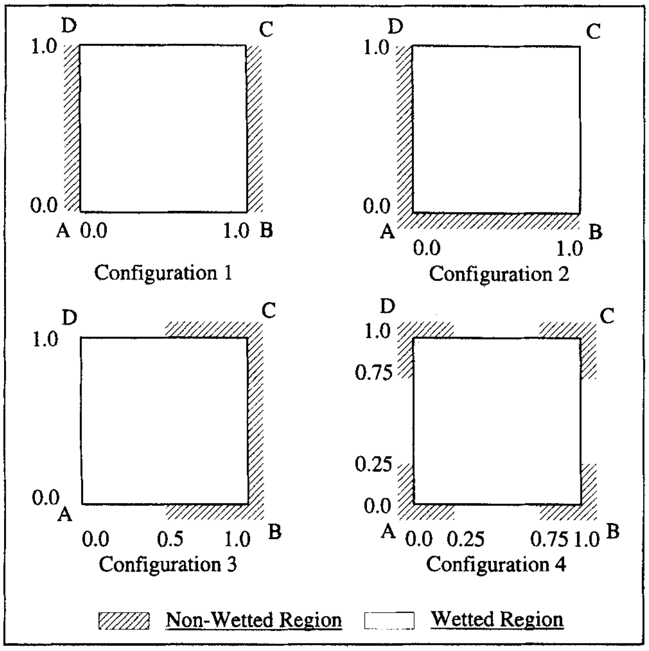

Figure 4. Four different wetting configurations for the same wetting efficiency in a slab catalyst particle.

Table 2. Yield of Intermediates for Different Wetting Configurations

Configuration	*B*	*C*	*D*
1	0.445	0.177	0.234
2	0.462	0.163	0.229
3	0.464	0.161	0.228
4	0.454	0.182	0.241

wetting configurations, the maximum difference being 13% between configurations 3 and 4 for component *C*. However, these results are specific to the chosen set of kinetic parameters.

Similar studies can be performed for several truncated schemes of Figure 5. For example, let us consider a simple series reaction subscheme from the reaction network 2:

$$A \xrightarrow{m_1^2} B \xrightarrow{m_2^2} E. \tag{38}$$

For the four wetting configurations shown in Figure 4, we study the effect of the parameter m_2 on the yield of B for a constant m_1 ($=1$). Figure 6 is a logarithmic plot of yield of B vs. the parameter m_2. For large values of m_2, there is practically no effect of wetting configuration on the yield of B. But for small values of m_2, the difference in yield of B between wetting configurations 3 and 4 is as high as 22%. In view of this large difference, it becomes important to incorporate the effects of wetting configurations in designing heterogeneous reactors and BEM provides a quantitative tool for such studies. Since it is difficult to estimate the wetting pattern inside a reactor *a priori* the numerical results are usually matched with the experimental data to deduce the wetting pattern indirectly.

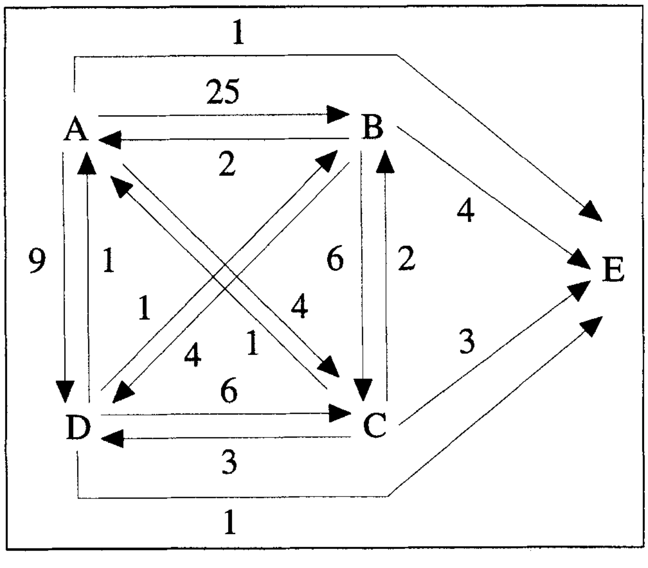

Figure 5. Reaction network 2.

Summary and Closure

The boundary element method is extended to analyze a network of linear diffusion reactions in two dimensions, and a systematic procedure is provided to calculate the key design parameters. The usefulness of the method to study the effect of catalyst geometry and nonuniform boundary conditions on the yield of intermediate products is demonstrated. The simulation results also indicate the possibility of altering the catalyst shape to enhance (decrease) the yield of a desired (undesired) product. Using the computational method discussed in this article, a rapid assessment of various catalyst shapes

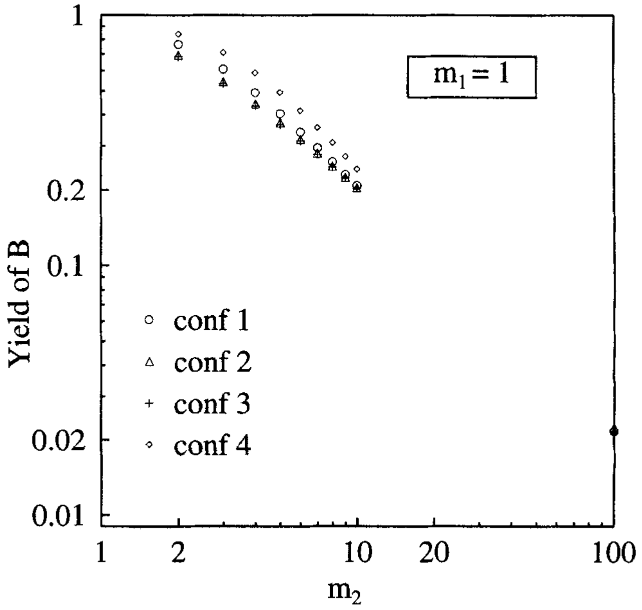

Figure 6. Effect of the parameter m_2 on the yield of B for the series reaction network given by Eq. 38.

can be made for a preliminary screening. The procedure is very general in nature and can be easily extended to 3-D problems by using the corresponding 3-D fundamental solution to the diffusion reaction operator and discretizing the surface of the particle. One application area is in the petroleum processing industry where multiple reactions are often encountered in non-regular catalyst geometries, often with nonuniform boundary conditions. For such problems, the computational methodology can be used to assess the diffusional effects and to arrive at an improved reactor design.

Notation

n = direction of outward normal
p = normal concentration gradient vector
x, y = spatial coordinates
π = constant = 3.141529

Subscripts

i = source point
k, m, l = species indices

Literature Cited

Aris, R., "On Shape Factors for Irregular Particles: I," *Chem. Eng. Sci.*, **6**, 262 (1957).

Brebbia, C. A., and J. Dominguez, *Boundary Elements—An Introductory Course*, Computational Mechanics Publications and McGraw Hill, New York (1989).

Cooper, B. H., B. B. L. Donnis and B. Moyse, "Hydroprocessing Conditions Affect Catalyst Shape Selection," *Oil Gas J.*, **84**, 39 (1986).

Funk, G. A., M. P. Harold, and K. M. Ng, "Effectiveness of a Partially Wetted Catalyst for Bimolecular Reaction Kinetics," *AIChE J.*, **34** (8), 1361 (1988).

Harold, M. P., "Impact of Wetting on Catalyst Performance in Multiphase Reaction Systems," in *Computer-Aided Design of Catalysts*, E. R. Becker and C. J. Pereira, eds., Marcel Dekker, New York, p. 391 (1993).

Karur, S. R., and P. A. Ramachandran, "Orthogonal Collocation in the Non-conforming Boundary Element Method," *J. Comput. Phy.*, **12**, 373 (1995).

Mills, P. L., and M. P. Duduković, "A Dual-Series Solution for the Effectiveness Factor of Partially Wetted Catalysts in Trickle-Bed Reactors," *Ind. Eng. Chem. Fundam*, **18**, 139 (1979).

Power, H., and P. W. Partridge, "The Use of Stokes' Fundamental Solution for the Boundary Only Element Formulation of the Three-Dimensional Navier-Stokes Equations for Moderate Reynolds Numbers," *Int. J. Num. Meth. Eng.*, **37**, 1825 (1994).

Pozrikidis, C., *Boundary Integral and Singularity Methods for Linearized Viscous Flow*, Cambridge Univ. Press, Cambridge, England (1992).

Ramachandran, P. A. and J. M. Smith, "Effectiveness Factors in Trickle Bed Reactors," *AIChE J.*, **25**, 538 (1979).

Ramachandran, P. A., "Boundary Integral Element Method for Linear Diffusion-Reaction Problems with Discontinuous Boundary Conditions," *Chem. Eng. J.*, **47**, 169 (1991).

Ramachandran, P. A., *Boundary Element Methods in Transport Phenomena*, Computational Mechanics, Southampton, England (1994).

Sie, S. T., "Intraparticle Diffusion and Reaction Kinetics as Factors in Catalyst Particle Design," *Chem. Eng. J.*, **53**, 1 (1993).

Stangeland, B. E., and J. R. Kittrel, "Jet Fuel Selectivity in Hydrocracking," *Ind. Eng. Chem. Proc. Des. Dev.*, **11**, 15 (1972).

Wei, J., and C. D. Prater, "The Structure and Analysis of Complex Reaction Systems," *Advances in Catalysis*, Vol. 13, Academic Press, New York, p. 203 (1962).

Yentekakis, I. V., and C. G. Vayenas, "Effectiveness Factors for Reactions between Volatile and Non-Volatile Components in Partially Wetted Catalysts," *Chem. Eng. Sci.*, **42**, 1323 (1987).

Manuscript received Jan. 3, 1995, and revision received Apr. 3, 1995.